Journal of Visualized Experiments

A time-efficient fluorescence spectroscopy-based assay for evaluating actin polymerization status in rodent and human brain tissues

--Manuscript Draft--

Article Type:	Invited Methods Collection - Author Produced Video
Manuscript Number:	JoVE62268R2
Full Title:	A time-efficient fluorescence spectroscopy-based assay for evaluating actin polymerization status in rodent and human brain tissues
Corresponding Author:	Faraz Ahmad University of Otago Dunedin, Otago NEW ZEALAND
Corresponding Author's Institution:	University of Otago
Corresponding Author E-Mail:	faraz.ahmad@otago.ac.nz
Order of Authors:	Faraz Ahmad
	Ping Liu
Additional Information:	
Question	**Response**
Please indicate whether this article will be Standard Access or Open Access.	Standard Access (US$1200)
Please specify the section of the submitted manuscript.	Neuroscience
Please confirm that you have read and agree to the terms and conditions of the author license agreement that applies below:	I agree to the Author License Agreement
Please provide any comments to the journal here.	
Please indicate whether this article will be Standard Access or Open Access.	Standard Access ($1400)

TITLE:

A Time-Efficient Fluorescence Spectroscopy-Based Assay for Evaluating Actin Polymerization Status in Rodent and Human Brain Tissues

AUTHORS AND AFFILIATIONS:

Faraz Ahmad[1], Ping Liu[1]

[1]Department of Anatomy, School of Biomedical Sciences, University of Otago, Dunedin, New Zealand

Corresponding Authors:
Faraz Ahmad
faraz.ahmad@otago.ac.nz

Ping Liu
ping.liu@otago.ac.nz

KEYWORDS:

synaptosomes, synaptoneurosomes, F-actin, cytoskeleton, depolarization, latrunculin A, phalloidin, fluorescence.

SUMMARY:

We report a simple, time-efficient and high-throughput fluorescence spectroscopy-based assay for the quantification of actin filaments in *ex vivo* biological samples from brain tissues of rodents and human subjects.

ABSTRACT:

Actin, the major component of cytoskeleton, plays a critical role in the maintenance of neuronal structure and function. Under physiological states, actin occurs in equilibrium in its two forms: monomeric globular (G-actin) and polymerized filamentous (F- actin). At the synaptic terminals, actin cytoskeleton forms the basis for critical pre- and post-synaptic functions. Moreover, dynamic changes in the actin polymerization status (interconversion between globular and filamentous forms of actin) are closely linked to plasticity-related alterations in synaptic structure and function. We report here a modified fluorescence-based methodology to assess polymerization status of actin in *ex vivo* conditions. The assay employs fluorescently labelled phalloidin, a phallotoxin that specifically binds to actin filaments (F-actin), providing a direct measure of polymerized filamentous actin. As a proof of principle, we provide evidence for the suitability of the assay both in rodent and post-mortem human brain tissue homogenates. Using latrunculin A (a drug that depolymerizes actin filaments), we confirm the utility of the assay in monitoring alterations in F-actin levels. Further, we extend the assay to biochemical fractions of isolated synaptic terminals wherein we confirm increased actin polymerization upon stimulation by depolarization with high extracellular K^+.

INTRODUCTION:

Cytoskeletal protein actin is involved in multiple cellular functions, including structural support, cellular transport, cell motility and division. Actin occurs in equilibrium in two forms: monomeric globular actin (G-actin) and polymerized filamentous actin (F-actin). Rapid changes in the polymerization status of actin (interconversion between its G- and F- forms) result in rapid filament assembly and disassembly and underlie its regulatory roles in cellular physiology. Actin forms the major component of the neuronal cytoskeletal structure and influences a wide range of neuronal functions[1, 2]. Of note, the actin cytoskeleton forms an integral part of the structural platform of the synaptic terminals. As such, it is a major determinant of synaptic morphogenesis and physiology and plays a fundamental role in control of the size, number and morphology of synapses[3–5]. In particular, dynamic actin polymerization-depolymerization is a key determinant of the synaptic remodelling associated with synaptic plasticity underlying the memory and learning processes. Indeed, both presynaptic (such as neurotransmitter release[6–10]) and postsynaptic functions (plasticity related dynamic remodeling[11–14]) critically rely on dynamic changes in the polymerization status of the actin cytoskeleton.

Under physiological conditions, F-actin levels are dynamically and tightly regulated through a multimodal pathway involving posttranslational modification[4, 15, 16] as well as actin-binding proteins (ABPs)[4, 17]. ABPs can influence actin dynamics at multiple levels (such as initiating or inhibiting polymerization, inducing filament branching, severing of filaments to smaller pieces, promoting depolymerization, and protecting against depolymerization), and are in-turn under a stringent modulatory control sensitive to various extra- and intracellular signals[18–20]. Such regulatory checks at multiple levels dictate a strict regulation of actin dynamics at the synaptic cytoskeleton, fine-tuning pre- and postsynaptic aspects of neuronal physiology both at the basal and activity-induced states.

Given the important roles of actin in neuronal physiology, it is not surprising that several studies have provided evidence for alterations in actin dynamics as critical pathogenic events linked to a wide range of neurological disorders including neurodegeneration, psychological diseases as well as neurodevelopmental ailments[3, 21–27]. In spite of the wealth of research data pointing to key roles of actin in neuronal physiology and pathophysiology, however, significant gaps still remain in the understanding of actin dynamics, particularly at the synaptic cytoskeleton. More research studies are needed to have a better comprehension of neuronal actin and its alterations under pathological conditions. One major area of focus in this context is the assessment of actin polymerization status. There are Western blotting-based commercial kits (G-Actin/F-Actin in vivo assay biochemical kit; Cytoskeleton SKU BK037[28, 29]) and home-made assays for the assessment of F-actin levels[6]. However, because these require biochemical isolation of F-actin and G-actin and because their subsequent quantification is based upon immunoblotting protocols, they can be time consuming. We herein report a fluorescence spectroscopy-based assay adapted from a previous study[30] with modifications that can be used to evaluate both basal levels of F-actin, as well as dynamic changes in its assembly-disassembly. Notably, we have efficiently modified the original protocol that requires samples suitable for a 1 mL cuvette to the current 96-well plate format. The modified protocol has therefore significantly reduced the tissue/sample amount required for the assay. Further, we provide evidence that the protocol is suitable for not only brain tissue homogenates, but also subcellular fractions such as isolated synaptic terminals

(synaptosomes and synaptoneurosomes). Lastly, the assay can be employed for freshly dissected rodent brain tissues and long-term stored post-mortem human brain samples. Of note, while the assay is presented in a neuronal context, it can be suitably extended to other cell-types and physiological processes associated with them.

PROTOCOL:

All experimental procedures were carried out in accordance with the regulations of the University of Otago Committee on Ethics in the Care and Use of Laboratory Animals (Ethics Protocol No. AUP95/18 and AUP80/17) and New Zealand legislature. Human brain tissues were obtained from the Neurological Tissue Bank of Hospital Clínic-IDIBAPS BioBank in Barcelona, Spain. All tissue collection protocols were approved by the Ethics Committee of Hospital Clínic, Barcelona, and informed consent was obtained from the families.

1. Preparation of buffers and reagents

1.1. Prepare the following buffers for the homogenization of brain tissue and the preparation of enriched fraction of synaptic terminals:
Homogenization buffer: 5 mM HEPES, pH 7.4 supplemented with 0.32 M sucrose
Resuspension buffer: 5 mM Tris, pH 7.4 supplemented with 0.32 M sucrose
Washing buffer: 5 mM Tris, pH 8.1
1.2 M sucrose
1.0 M sucrose
0.85 M sucrose

1.2. Add homemade or commercial mix of protease and phosphatase inhibitors.

NOTE: We have used EDTA-free version of Complete Protease Inhibitor mix (1 tablet per 10 mL buffer) and Phosphatase inhibitor cocktail IV (1:100; volume: volume).

1.3. Prepare the following buffers and reagents for the fixation, permeabilization and binding of phalloidin:
Krebs buffer: 118.5 mM NaCl, 4.7 mM KCl, 1.2 mM $MgCl_2$, 2 mM $CaCl_2$, 0.1 mM KH_2PO_4, 5 mM $NaHCO_3$, 10 mM glucose, 20 mM HEPES, pH 7.4
1 M KCl
25% glutaraldehyde (stock solution)
Krebs buffer containing 0.1 % Triton X-100 and 1 mg/mL $NaBH_4$
400x Alexa Fluor 647 Phalloidin in DMSO
Krebs buffer containing 0.32 M sucrose
50 μM latrunculin A in DMSO (stock solution)
1 M KCl (stock solution)

CAUTION: Phalloidin is toxic (LD_{50} = 2 mg/kg) and must be handled with care. Inhalation of glutaraldehyde is toxic and should be handled in a fume hood.

1.4. Store the buffers at 4 °C and phalloidin and latrunculin A at -20 °C for long-term storage.

NOTE: Long-term storage of buffers is not recommended. The protocol can be paused here.

2. Brain tissue homogenization

2.1. Homogenize the cryopreserved or freshly dissected rat brain tissue in 10 volumes of homogenization buffer in a Potter-*Elvehjem* glass tube and pestle on ice.

NOTE: Optimal homogenization is achieved by 15-20 strokes of the pestle by hand for brain tissues. Successful homogenization can be confirmed by smooth flow of the suspension through the glass tube. The protocol can be paused here.

2.2. Determine the protein concentration in the homogenate using a Bradford assay[31].

NOTE: Alternate home-made or commercial assays for protein estimation can also be used.

2.3. Dilute homogenate samples in Krebs buffer at a concentration of 2-3 mg protein/mL in a volume of 50 µL.

NOTE: In some of our experiments, we incubate homogenates with 2 µM latrunculin A or DMSO (controls) at 37 °C for 1 h. For this, homogenates are resuspended in 48 µL of Krebs buffer, and 2 µL of 50 µM latrunculin A or 2 µL of DMSO is added. Further for immunoblotting, a small amount of sample (2 µg) is collected after the incubation.

2.4. Fix the homogenate samples (section 5).

3. Preparation of isolated nerve terminals

3.1. Preparation of synaptosomes

NOTE: Alternative protocols[32, 33] for synaptosomes can also be used.

3.1.1. Centrifuge brain homogenate at 1,200 x *g* for 10 min at 4 °C.

3.1.2. Discard the pellet, which is the crude nuclear fraction.

3.1.3. Further centrifuge the supernatant (S1) obtained in step 3.1.1 at 12,000 x g for 15 min at 4 °C.

3.1.4. Remove the supernatant (S2), which is the soluble cytosolic fraction.

3.1.5. Resuspend the pellet (P2) obtained in step 3.1.3, which is the crude synaptosomal fraction in resuspension buffer.

NOTE: The volume of resuspension buffer depends on the amount of starting tissue and the amount of pellet obtained. For example, when starting with 150-300 mg of brain tissues, the pellet obtained can be resuspended in 200 µL of resuspension buffer.

3.1.6. Load the resuspended crude synaptosomes onto a discontinuous sucrose gradient made of equal volumes of 0.85-1.0-1.2 M sucrose.

NOTE: We typically use 1 mL each of the sucrose solution (for 150-300 mg tissue). This can be changed according for larger tissue amounts. Discontinuous gradients can be made using a 25G syringe pressed against the internal wall of the ultracentrifuge tube and gentle layering of the sucrose layers.

3.1.7. Centrifuge at 85,000 x g for 2 h at 4 °C.

NOTE: Because of the high-speed of centrifugation, an ultracentrifuge capable of creating a vacuum to reduce heating is required.

3.1.8. Collect the synaptosomal fraction at the interface between 1.0 and 1.2 M sucrose using a 200 µL pipet tip.

3.1.9. Wash the synaptosomal fraction with washing buffer by centrifugation at 18,000 x g for 10 minutes at 4 °C.

NOTE: For washing, the synaptosomal fraction obtained at the interface of 1.0 and 1.2 M sucrose is collected in a fresh 1.5 mL tube, and an equal volume of washing buffer is added, ensuring the removal of high sucrose from the medium.

3.1.10. Wash the synaptosomal pellet again with homogenization buffer.

3.1.11. Resuspend the synaptosomes in homogenization buffer on ice.

NOTE: The protocol can be briefly paused here.

3.1.12. Determine the protein concentration using a Bradford assay.

3.1.13. Resuspend the synaptosomes in Krebs buffer at a concentration of 2-3 mg protein/mL in a volume of 50 µL (47.5 µL if synaptosomes are to be depolarized by KCl; see section 4).

NOTE: For resuspension, the synaptosomal fraction is first spun at 12,000 x g for 5 min at 4 °C and the supernatant (buffer) is removed. The synaptosomal pellet is then resuspended in Krebs buffer by gentle pipetting using a 200 µL pipet tip.

3.1.14. Proceed with depolarization (section 4).

3.2. Preparation of synaptoneurosomes

NOTE: Alternative protocols[34, 35] for synaptoneurosomes can also be used.

3.2.1. Pass the brain homogenate through a pre-wetted net filter of 100 μm pore size in a filter holder using a 1 mL syringe.

NOTE: Pre-wetting of all filters is important to avoid loss of sample and should be done using homogenization buffer. For this, homogenization buffer is passed through the filters in the filter holder using a 1 mL syringe making until the buffer can be seen coming out.

3.2.2. Collect the filtrate (F1) in a pre-chilled 1.5 mL tube on ice.

3.2.3. Repeat the process for F1 fraction to obtain the second filtrate (F2).

3.2.4. Pass F2 filtrate through a net filter of 5 μm pore size.

3.2.5. Collect the filtrate (F3) in a pre-chilled 1.5 mL tube on ice.

3.2.6. Centrifuge filtrate F3 at 1,500 x g for 10 min at 4 °C.

3.2.7. Resuspend the pellet (synaptoneurosomes) in Krebs buffer on ice at a concentration of 2-3 mg protein/mL in a volume of 50 μL (47.5 μL if synaptosomes are to be depolarized by KCl; see section 4).

NOTE: The protocol can be briefly paused here.

3.2.8. Estimate the protein concentration using a Bradford assay.

3.2.9. Proceed with depolarization (section 4).

4. KCl-mediated depolarization of isolated synaptic terminals

4.1. Equilibrate synaptosomes/synaptoneurosomes at 37 °C for 5-10 min.

4.2. Stimulate synaptosomes/synaptoneurosomes by adding KCl to increase extracellular K^+ to 50 mM for 30 s at 37 °C and add equal volume of Krebs buffer to the respective unstimulated control set.

NOTE: For example, add 2.5 μL of 1 M KCl to synaptosomes resuspended in 47.5 μL of Krebs buffer; and add 2.5 μL of Krebs buffer to the respective unstimulated control synaptosome. For

experiments wherein a large number of samples are involved, proceed with no more than 2 samples at a time so that the depolarization time does not exceed 30 s.

4.3. Terminate stimulation by adding glutaraldehyde (section 5).

5. Fixation and phalloidin staining of samples

5.1. Add glutaraldehyde to homogenate/synaptosomal/synaptoneurosomal samples to a final concentration of 2.5% for 2-3 min at room temperature.

NOTE: We added 6 µL of 25% glutaraldehyde solution so that the final concentration of glutaraldehyde in the 50 µL samples (homogenates/synaptosomes/synaptoneurosomes) was ca. 2.5%. Fixation is critical and should be fast and hence immediately after adding glutaraldehyde, the sample should be vigorously vortexed.

5.2. Sediment the samples at 20,000 x g for 5 min.

5.3. Remove the supernatant.

NOTE: Discard the supernatant in a fume hood as glutaraldehyde is toxic.

5.4. Permeabilize the pellet by resuspension in 100 µL of Krebs buffer containing 0.1% Triton X-100 and 1 mg/mL $NaHB_4$ for 2-3 min at room temperature.

5.5. Sediment the samples at 20,000 x g for 5 min.

5.6. Remove the permeabilization buffer.

5.7. Wash the pellet with 200 µL of Krebs buffer by centrifuging at 20,000 x g for 5 min.

5.8. Resuspend and stain the pellet with 1x Alexa Fluor 647 Phalloidin (corresponding to 500 µU) in 100 µL of Krebs buffer for 10 minutes in dark at room temperature.

NOTE: Other varieties of fluorescent phalloidin analogs are commercially available and can be replaced for the assay. Concentration of phalloidin and total sample volume of incubation may have to be modified according to the amount and type of tissue/sample being tested and optimal conditions should be standardized accordingly.

5.9. Centrifuge the stained samples at 20,000 x g for 5 min.

5.10. Remove the unbound phalloidin (supernatant).

5.11. Wash the sample with 200 µL of Krebs buffer by centrifugation at 20,000 x g for 5 min.

5.12. Resuspend in 200 µL of Krebs buffer containing 0.32 M sucrose.

NOTE: The protocol can be briefly paused here.

6. Fluorometric analysis and light scattering

6.1. Dispense Alexa Fluor 647 Phalloidin-stained samples in a black 96-well plate.

6.2. Measure the fluorescence intensity at an excitation wavelength of 645 nm and an emission wavelength of 670 nm in a plate reader at room temperature.

6.3. Transfer the samples from the black 96-well plate to the transparent 96-well plate using 200 µL pipet tips.

6.4. Measure the light scattering at 540 nm to correct for any losses that might have occurred during the previous steps of fixation, permeabilization and staining.

NOTE: Variations in biological material retained in the stained samples might be more prominent for smaller amounts of starting material (see Discussion).

6.5. Include a set of Alexa Fluor 647 Phalloidin in Krebs buffer at different concentrations (0.05x, 0.1x, 0.25x, 0.35x, 0.75x, 0.5x and 1x corresponding to 25, 50, 125, 175, 250, 375 and 500 µU) for each batch of the assay as a standard curve.

NOTE: This is an optional step and does not affect the results of the assay particularly when F-actin levels are being expressed in a relative manner (Section 7). The protocol can be paused here.

7. Data analysis

7.1. The amount of F-actin in the samples is directly proportional to the fluorescence intensity of bound phalloidin. Express in absolute terms of units of phalloidin bound calculated from the linear curve of the tagged phalloidin standard.

NOTE: As an example, see **Figures 2A-B, 3A, 4A-B** and **Supplementary Figure 2**.

7.2. Express F-actin levels as a fraction of the control samples.

NOTE: As an example, see **Figures 5A-B**.

REPRESENTATIVE RESULTS:

Linearity of the assay for evaluation of F-actin levels

First, a standard curve for the linear increase in fluorescence of Alexa Fluor 647 Phalloidin was ascertained and was repeated for each set of experiments (**Figure 1**). To investigate the linear

range of the assay, different amounts of brain homogenates from rodents (**Figures 2A and 2B**) and post-mortem human subjects (**Figure 3A and 3B**) were processed. The assay was found to be linear in the range of 50-200 μg of protein as assessed by amounts of labeled phalloidin retained. Light scattering at 540 nm was used to confirm the different amounts of samples (**Figure 2C** and **Figure 3C**).

Latrunculin, an actin depolymerizing agent reduces binding of labelled phalloidin

Latrunculin A is known to depolymerize actin filaments and reduce the levels of F-actin[36–39]. Homogenates from either rodent or human brain tissues were incubated with 2 μM latrunculin A for 1 hour at 37 °C to depolymerize actin filaments. Respective untreated control sets were incubated with DMSO for the same duration of 1 hour at 37 °C. The assay robustly measured the loss of F-actin levels from 95.7 ± 6.6 (mean ± SEM) in control samples to 72.0 ± 3.2 (mean ± SEM) μU of bound phalloidin in latrunculin A-treated samples in rodent brain homogenates (**Figure 4A**). A similar decrease (from 83.7 ± 3.9 to 66.9 ± 4.2 μU) in retention of labeled phalloidin was also observed when homogenates from human brain tissues were subjected to latrunculin A treatment (**Figure 4B**). Noteworthy, total actin levels, as assessed by immunoblotting, did not alter upon treatment with latrunculin A in both rat (**Supplementary Figure 1A-B**) and human (**Supplementary Figure 1C-D**) brain homogenates.

Depolarization of isolated synaptic terminals stimulates actin polymerization and filament formation

Ex vivo depolarization of isolated synaptic terminals has been shown to result in rapid stimulation of actin polymerization[6, 30, 40], and this phenomenon was used as a further confirmation of the assay reported herein. Biochemical fractions enriched in synaptic terminals were prepared in two different manners; a gradient-based ultracentrifugation method to obtain "synaptosomes"[41–44] and a sequential filtration-based protocol to obtain "synaptoneurosomes"[43, 45, 46]. Because the yield for the latter is higher, we used it for human post-mortem brain tissues wherein the tissue amounts are often limiting. On the other hand, we preferred to use synaptosomes with a higher degree of enrichment of synaptic fragments[41] for our rat brain tissue experiments.

Depolarization of synaptosomes or synaptoneurosomes and stimulation of actin polymerization were achieved by a short (30 second) burst of increase in extracellular K^+ to 50 mM. KCl exposure resulted in increased phalloidin binding by almost 40% in rodent brain synaptosomes compared to the respective mock-stimulated controls (**Figure 5A**; see also **Supplementary Figure 2A**). A smaller (around 20%) but consistent increase was also observed in human synaptoneurosomes treated with KCl (**Figure 5B**; see also **Supplementary Figure 2A**). These experiments validate the robustness of our assay in determining alterations in F-actin levels in brain tissue samples, including isolated synaptic terminals.

FIGURE AND TABLE LEGENDS:

Figure 1. Standard curve for fluorescence of Alexa Fluor 647 Phalloidin.

Linearity of fluorescence emission of different amounts (25-500 μU) of labeled phalloidin was confirmed by fluorescence spectroscopy at an excitation of 645 nm and emission of 670 nm (R^2

= 0.9942). Data are represented as mean ± SEM (n=3).

Figure 2. Linearity of phalloidin binding to whole-cell homogenates from rat brain tissue.
(**A**) Binding of phalloidin to different amounts of homogenates (50-300 μg protein) was assessed. (**B**) Binding was linear in the range of 50-200 μg protein (R^2 = 0.9602). (**C**) Scattering at 540 nm was used to confirm different amounts of the samples (R^2 = 0.8319). Data are represented as mean ± SEM (n=4).

Figure 3. Phalloidin binding to whole-cell homogenates from post-mortem human brain tissue.
(**A**) Phalloidin retention in a range of amounts of homogenates (50-300 μg protein) was evaluated. (**B**) Phalloidin binding was found to be linear in the range of 50-200 μg protein (R^2 = 0.8832). (**C**) Scattering at 540 nm confirmed the varying amounts of the samples (R^2 = 0.9730). Data are represented as mean ± SEM (n=4).

Figure 4. Effects of latrunculin A on F-actin levels.
Treatment of brain homogenates with actin depolymerizing agent Latrunculin A (2 μM, 1 h at 37°C) resulted in significant decrease in the amounts of actin filaments compared to the respective mock-treated control samples as assessed by retention of labeled phalloidin both in rodent (p = 0.0034; paired two-tailed Student's *t*-test) (**A**) and post-mortem human tissues (p = 0.0011; paired two-tailed Student's *t*-test) (**B**). Data are represented as mean ± SEM (n=6 pairs).

Figure 5. Effects of KCl-mediated depolarization on F-actin amounts in isolated synaptic terminals.
(**A**) Incubation of synaptosomes from rat brain with 50 mM KCl for 30 s at 37°C stimulated actin polymerization which consequently resulted in an increase in phalloidin binding (p = 0.0014; paired two-tailed Student's *t*-test). (**B**) A smaller increase was also observed in synaptoneurosomal fraction from post-mortem human brain tissues (p = 0.014; paired two-tailed Student's *t*-test). Data are represented as mean ± SEM (n=6 pairs).

Supplementary Figure 1. Effects of latrunculin A on total actin levels.
Brain homogenates were incubated with latrunculin A (2 μM, 1 h at 37°C) or equal volume of DMSO (1 h at 37°C). 10 μg protein per sample (latrunculin A treated and DMSO mock-treated controls) were collected prior to fixation. Total actin levels were assessed by immunoblotting. Representative blots are shown for rat (**A**) and human (**C**) brain homogenates. Latrunculin A did not alter the total actin levels in both rat (**B**; p = 0.40; paired two-tailed Student's *t*-test) and human (**D**; p = 0.42; paired two-tailed Student's *t*-test) brain homogenates. Data are represented as mean ± SEM (n=3 pairs).

Supplementary Figure 2. Effects of KCl-mediated depolarization on F-actin levels in rat synaptosomes and human synaptoneurosomes.
(**A**) Incubation of synaptosomes from rat brain with 50 mM KCl (30 s at 37 °C) stimulated actin polymerization and a consequent increase in phalloidin binding (p = 0.0019; paired two-tailed Student's *t*-test). (**B**) Increase in phalloidin retention was also observed in human

synaptoneurosomal fraction depolarized by KCl compared to the respective unstimulated controls ($p = 0.015$; paired two-tailed Student's *t*-test). Data are represented as mean ± SEM (n=6 pairs).

DISCUSSION:

The assay described here, essentially adapted from a previous study[30] with modifications, employs a phallotoxin, phalloidin tagged with a fluorescent label. Fluorescent phalloidin analogs are considered to be the gold standard for staining actin filaments in fixed tissues[47–49]. In fact, they are the oldest tools to specifically identify actin filaments[50] and still remain the most widely used instruments to detect actin filaments particularly for subsequent fluorescence microscopy-based analyses. Importantly, phalloidin has been shown to stain even loose, irregular meshwork of short actin filaments[51], indicating that phalloidin binding is not dependent on the filament length. Our protocol, on the other hand, relies on fluorescence spectroscopy to analyze actin dynamics in *ex vivo* biological samples, for example brain tissues from rodents and humans.

The major advantage of the protocol is that it considerably reduces the time taken with respect to the existing protocols that first require a high-speed centrifugation-based biochemical isolation of F-actin (separation from G-actin based on insolubility of actin filaments in certain detergents such as Triton X-100) and subsequent analysis of immunoreactive levels using Western blotting[6, 28, 29]. The time-efficiency of our assay is also an advantage with regards to phalloidin-based immunocytochemistry techniques[40, 52], although there might be some other benefits associated with the latter. Another advantage is that it can be applied to cryopreserved post-mortem human brain tissues, procurement of which is always associated with some post-mortem delay. Further, with respect to the original protocol[30] from which this methodology has been modified, we have considerably reduced the requirement for the tissue amount from 1 mL cuvette to a single well of a 96-well plate. Moreover, because of the inclusion of a phalloidin standard curve in each set of experiment, our protocol can quantitate absolute levels of actin filaments in units of phalloidin bound (**Figures 2A-B, 3A, 4A-B;** see also **Supplementary Figure 2**), as well as the levels relative to control samples (**Figure 5A-B**).

It should be noted that the application of phalloidin to assess F-actin levels however is restricted to fixed cells and samples, both for our assay protocol as well as microscopy-based protocols. This is because phalloidin is essentially a toxic bicyclic heptapeptide that binds specifically at the interface between F-actin subunits with high affinity and stabilizes these actin filaments, rendering them incapable to depolymerize and in fact increasing the net conversion of G-actin into F-actin[40, 53, 54]. Hence, phalloidin stabilizes actin filaments *in vivo* and *in vitro*, and can result in significant changes in the equilibrium status of actin *per se*[47, 55]. As such evaluation of actin polymerization status mediated by fluorescent phalloidin is based upon arrested filament structures. Moreover, because of its low permeability through the lipid bilayer, phalloidin-based methodologies rely on permeabilization of the cells or biological samples. Infeasibility of a time course live-cell assay is hence a major limitation of the protocol as with immunocytochemistry-based methods employing phalloidin.

Infeasibility of phalloidin-based methods to evaluate dynamic changes in actin filaments in live

unfixed cells begs the question of whether there are alternative procedures to do so. Indeed, advances have been made in this regard with exogenous expression of fluorescent-actin analogs prior to analysis using protocols such as video micrography[36, 56], fluorescence recovering after photobleaching (FRAP)[38] or fluorescence resonance energy transfer (FRET)[39]. Heterologous expression of fluorescently tagged peptides and proteins that bind actin filaments are also employed to study actin dynamics in live cells; however there are disadvantages and limitations associated with them as well as with the heterologous expression of fluorescently tagged actin[47, 49, 57]. For example, G-actin that comprises 50-70% of total actin in most cells is soluble and freely diffusible in the cytosol, resulting in a higher background causing challenges in differentiating signals from actin filaments specifically[57].

A critical factor in the assay is that as shown in **Figure 2** and **Figure 3**; it is not linear throughout the range of protein amounts tested. Hence, an optimal amount of protein suitable for the assay should be determined first or the amount of phalloidin analog should be adjusted such that it is no longer limiting (at higher amounts of proteins). Another critical aspect of the protocol is that the multiple centrifugation-based steps for removal of fixative, permeabilization agent and unbound phalloidin can lead to varying loss of proteins (and F-actin bound phalloidin) from the samples, particularly when lower amounts of samples are used. Hence it is important to normalize the amount of sample retained by monitoring light scattering at 540 nm. Lastly, since actin is in a dynamic state of interconversion between its F- and G-forms, fixing should be fast. A minor related critical aspect of the assay is that we could not evaluate its efficiency in assessing pharmacological actin polymerization. As opposed to pharmacological actin depolymerization by latrunculin A, jasplakinolide (a reliable and widely used actin polymerizing agent) has overlapping binding sites with phalloidin and competitively inhibits its binding to actin filaments[58, 59]. Nevertheless, employment of KCl-stimulated synaptic terminals as an *ex vivo* model for increased actin polymerization indicates that our assay can also detect increases in F-actin levels.

In conclusion, we describe a robust time-efficient and high-throughput assay for analysis of actin filaments (F-actin) and its alternations in physiological and pathophysiological states suitable for a 96-well plate format. In combination with other existing methods for evaluation of F-actin in fixed and unfixed samples, the protocol will prove to be an essential tool in actin-related studies in the neuroscience field, as well as other areas of biological science research.

ACKNOWLEDGMENTS:

This work was supported by the Neurological Foundation of New Zealand (1835-PG), the New Zealand Health Research Council (#16-597) and the Department of Anatomy, University of Otago, New Zealand. We are indebted to the Neurological Tissue Bank of HCB-IDIBAPS BioBank (Spain) for human brain tissues. We thank Jiaxian Zhang for her help in recording and editing of the video.

DISCLOSURES:

The authors have nothing to disclose.

REFERENCES:

1. Penzes, P., Rafalovich, I. Regulation of the actin cytoskeleton in dendritic spines. *Advances*

in Experimental Medicine and Biology. **970**, 81–95, doi: 10.1007/978-3-7091-0932-8_4 (2012).
2. Venkatesh, K., Mathew, A., Koushika, S.P. Role of actin in organelle trafficking in neurons. *Cytoskeleton*. **77** (3–4), 97–109, doi: 10.1002/cm.21580 (2020).
3. Shirao, T., González-Billault, C. Actin filaments and microtubules in dendritic spines. *Journal of Neurochemistry*. **126** (2), 155–164, doi: 10.1111/jnc.12313 (2013).
4. Bertling, E., Hotulainen, P. New waves in dendritic spine actin cytoskeleton: From branches and bundles to rings, from actin binding proteins to post-translational modifications. *Molecular and Cellular Neuroscience*. **84**, 77–84, doi: 10.1016/j.mcn.2017.05.002 (2017).
5. Bellot, A. et al. The structure and function of actin cytoskeleton in mature glutamatergic dendritic spines. *Brain Research*. **1573**, 1–16, doi: 10.1016/j.brainres.2014.05.024 (2014).
6. Wolf, M. et al. ADF/Cofilin controls synaptic actin dynamics and regulates synaptic vesicle mobilization and exocytosis. *Cerebral Cortex*. **25** (9), 2863–75, doi: 10.1093/cercor/bhu081 (2015).
7. Morales, M., Colicos, M.A., Goda, Y. Actin-dependent regulation of neurotransmitter release at central synapses. *Neuron*. **27** (3), 539–550, doi: 10.1016/S0896-6273(00)00064-7 (2000).
8. Doussau, F., Augustine, G.J. The actin cytoskeleton and neurotransmitter release: An overview. *Biochimie*. **82** (4), 353–363, doi: 10.1016/S0300-9084(00)00217-0 (2000).
9. Sakaba, T., Neher, E. Involvement of actin polymerization in vesicle recruitment at the calyx of held synapse. *Journal of Neuroscience*. doi: 10.1523/jneurosci.23-03-00837.2003 (2003).
10. Lee, J.S., Ho, W.K., Lee, S.H. Actin-dependent rapid recruitment of reluctant synaptic vesicles into a fast-releasing vesicle pool. *Proceedings of the National Academy of Sciences of the United States of America*. doi: 10.1073/pnas.1114072109 (2012).
11. Rust, M.B. *et al.* Learning, AMPA receptor mobility and synaptic plasticity depend on n-cofilin-mediated actin dynamics. *EMBO Journal*. **29**, 1889–1902, doi: 10.1038/emboj.2010.72 (2010).
12. Bosch, M. et al. Structural and molecular remodeling of dendritic spine substructures during long-term potentiation. *Neuron*. **82**, 444–459, doi: 10.1016/j.neuron.2014.03.021 (2014).
13. Hanley, J.G. Actin-dependent mechanisms in AMPA receptor trafficking. *Frontiers in Cellular Neuroscience*. **8**, 381, doi: 10.3389/fncel.2014.00381 (2014).
14. Kasai, H., Fukuda, M., Watanabe, S., Hayashi-Takagi, A., Noguchi, J. Structural dynamics of dendritic spines in memory and cognition. *Trends in Neurosciences*. **33**, 121–129, doi: 10.1016/j.tins.2010.01.001 (2010).
15. Terman, J.R., Kashina, A. Post-translational modification and regulation of actin. *Current Opinion in Cell Biology*. **25** (1), 30–38, doi: 10.1016/j.ceb.2012.10.009 (2013).
16. Wilson, C., Terman, J.R., González-Billault, C., Ahmed, G. Actin filaments—A target for redox regulation. *Cytoskeleton*. **73**, 577–595, doi: 10.1002/cm.21315 (2016).
17. Borovac, J., Bosch, M., Okamoto, K. Regulation of actin dynamics during structural plasticity of dendritic spines: Signaling messengers and actin-binding proteins. *Molecular and Cellular Neuroscience*. **91**, 122–130, doi: 10.1016/j.mcn.2018.07.001 (2018).
18. Saneyoshi, T., Hayashi, Y. The Ca2+ and Rho GTPase signaling pathways underlying activity-dependent actin remodeling at dendritic spines. *Cytoskeleton*. **69** (8), 545–54, doi: 10.1002/cm.21037 (2012).
19. Mizuno, K. Signaling mechanisms and functional roles of cofilin phosphorylation and

570 dephosphorylation. *Cellular Signalling*. **25** (2), 457–69, doi: 10.1016/j.cellsig.2012.11.001 (2013).
571 20. Dos Remedios, C.G. *et al.* Actin binding proteins: Regulation of cytoskeletal
572 microfilaments. *Physiological Reviews*. **83** (2), 433–473, doi: 10.1152/physrev.00026.2002
573 (2003).
574 21. Bamburg, J.R., Bernstein, B.W. Actin dynamics and cofilin-actin rods in Alzheimer disease.
575 *Cytoskeleton*. **73** (9), 477–97, doi: 10.1002/cm.21282 (2016).
576 22. Penzes, P., VanLeeuwen, J.E. Impaired regulation of synaptic actin cytoskeleton in
577 Alzheimer's disease. *Brain Research Reviews*. **67** (1–2), 184–192, doi:
578 10.1016/j.brainresrev.2011.01.003 (2011).
579 23. Pelucchi, S., Stringhi, R., Marcello, E. Dendritic spines in Alzheimer's disease: How the
580 actin cytoskeleton contributes to synaptic failure. *International Journal of Molecular Sciences*. **21**
581 (3), 908, doi: 10.3390/ijms21030908 (2020).
582 24. Kounakis, K., Tavernarakis, N. The Cytoskeleton as a Modulator of Aging and
583 Neurodegeneration. *Advances in Experimental Medicine and Biology*. **1178**, 227–245, doi:
584 10.1007/978-3-030-25650-0_12 (2019).
585 25. Nishiyama, J. Plasticity of dendritic spines: Molecular function and dysfunction in
586 neurodevelopmental disorders. *Psychiatry and Clinical Neurosciences*. **73** (9), 541–550, doi:
587 10.1111/pcn.12899 (2019).
588 26. Michaelsen-Preusse, K., Feuge, J., Korte, M. Imbalance of synaptic actin dynamics as a key
589 to fragile X syndrome? *Journal of Physiology*. **596** (14), 2773–2782, doi: 10.1113/JP275571
590 (2018).
591 27. Hensel, N., Claus, P. The Actin Cytoskeleton in SMA and ALS: How Does It Contribute to
592 Motoneuron Degeneration? *Neuroscientist*. **24** (1), 54–72, doi: 10.1177/1073858417705059
593 (2018).
594 28. Kommaddi, R.P. *et al.* Aβ mediates F-actin disassembly in dendritic spines leading to
595 cognitive deficits in alzheimer's disease. *Journal of Neuroscience*. **38** (5), 1085–1099, doi:
596 10.1523/JNEUROSCI.2127-17.2017 (2018).
597 29. Kommaddi, R.P. *et al.* Glutaredoxin1 Diminishes Amyloid Beta-Mediated Oxidation of F-
598 Actin and Reverses Cognitive Deficits in an Alzheimer's Disease Mouse Model. *Antioxidants and*
599 *Redox Signaling*. **31** (18), 1321–1338, doi: 10.1089/ars.2019.7754 (2019).
600 30. Bernstein, B.W., Bamburg, J.R. Cycling of actin assembly in synaptosomes and
601 neurotransmitter release. *Neuron*. **3** (2), 257–265, doi: 10.1016/0896-6273(89)90039-1 (1989).
602 31. Sapan, C. V, Lundblad, R.L., Price, N.C. Colorimetric protein assay techniques.
603 *Biotechnology and applied biochemistry*. **29** (**Pt 2**) (2), 99–108, doi: 10.1111/j.1470-
604 8744.1999.tb00538.x (1999).
605 32. Kolodziej, A. *et al.* High resolution quantitative synaptic proteome profiling of mouse
606 brain regions after auditory discrimination learning. *Journal of Visualized Experiments*. **2016**
607 (118), 54992, doi: 10.3791/54992 (2016).
608 33. Byun, Y.G., Chung, W.S. A novel in vitro live-imaging assay of astrocyte-mediated
609 phagocytosis using pH indicator-conjugated synaptosomes. *Journal of Visualized Experiments*.
610 **2018** (132), 56647, doi: 10.3791/56647 (2018).
611 34. Chmielewska, J.J., Kuzniewska, B., Milek, J., Urbanska, K., Dziembowska, M. Neuroligin 1,
612 2, and 3 Regulation at the Synapse: FMRP-Dependent Translation and Activity-Induced
613 Proteolytic Cleavage. *Molecular Neurobiology*. **56** (4), 2741–2759, doi: 10.1007/s12035-018-

614 1243-1 (2019).
615 35. Kuzniewska, B., Chojnacka, M., Milek, J., Dziembowska, M. Preparation of polysomal
616 fractions from mouse brain synaptoneurosomes and analysis of polysomal-bound mRNAs.
617 *Journal of Neuroscience Methods*. **293**, 226–233, doi: 10.1016/j.jneumeth.2017.10.006 (2018).
618 36. Fischer, M., Kaech, S., Knutti, D., Matus, A. Rapid actin-based plasticity in dendritic spines.
619 *Neuron*. **20** (5), 847–854, doi: 10.1016/S0896-6273(00)80467-5 (1998).
620 37. Caesar, M., Felk, S., Aasly, J.O., Gillardon, F. Changes in actin dynamics and F-actin
621 structure both in synaptoneurosomes of LRRK2(R1441G) mutant mice and in primary human
622 fibroblasts of LRRK2(G2019S) mutation carriers. *Neuroscience*. **284**, 311–324, doi:
623 10.1016/j.neuroscience.2014.09.070 (2015).
624 38. Star, E.N., Kwiatkowski, D.J., Murthy, V.N. Rapid turnover of actin in dendritic spines and
625 its regulation by activity. *Nature Neuroscience*. **5**, 239–246, doi: 10.1038/nn811 (2002).
626 39. Okamoto, K.I., Nagai, T., Miyawaki, A., Hayashi, Y. Rapid and persistent modulation of
627 actin dynamics regulates postsynaptic reorganization underlying bidirectional plasticity. *Nature*
628 *Neuroscience*. **7**, 1104–1112, doi: 10.1038/nn1311 (2004).
629 40. Bernstein, B.W., Dewit, M., Bamburg, J.R. Actin disassembles reversibly during electrically
630 induced recycling of synaptic vesicles in cultured neurons. *Molecular Brain Research*. **53** (1–2),
631 236–250, doi: 10.1016/S0169-328X(97)00319-7 (1998).
632 41. Ahmad, F., Liu, P. Synaptosome as a tool in Alzheimer's disease research. *Brain Research*.
633 **1746**, 147009, doi: 10.1016/j.brainres.2020.147009 (2020).
634 42. Ahmad, F. *et al.* Isoform-specific hyperactivation of calpain-2 occurs presymptomatically
635 at the synapse in Alzheimer's disease mice and correlates with memory deficits in human
636 subjects. *Scientific Reports*. **8** (1), 13119, doi: 10.1038/s41598-018-31073-6 (2018).
637 43. Ahmad, F. *et al.* Reactive Oxygen Species-Mediated Loss of Synaptic Akt1 Signaling Leads
638 to Deficient Activity-Dependent Protein Translation Early in Alzheimer's Disease. *Antioxidants*
639 *and Redox Signaling*. **27** (16), 1269–1280, doi: 10.1089/ars.2016.6860 (2017).
640 44. Ahmad, F. *et al.* Developmental lead (Pb)-induced deficits in redox and bioenergetic status
641 of cerebellar synapses are ameliorated by ascorbate supplementation. *Toxicology*. **440**, 152492,
642 doi: 10.1016/j.tox.2020.152492 (2020).
643 45. Ahmad, F., Salahuddin, M., Alsamman, K., Herzallah, H.K., Al-Otaibi, S.T. Neonatal
644 maternal deprivation impairs localized de novo activity-induced protein translation at the
645 synapse in the rat hippocampus. *Bioscience Reports*. **38** (3), BSR20180118, doi:
646 10.1042/BSR20180118 (2018).
647 46. Ahmad, F., Salahuddin, M., Alsamman, K., Almulla, A.A., Salama, K.F. Developmental lead
648 (Pb)-induced deficits in hippocampal protein translation at the synapses are ameliorated by
649 ascorbate supplementation. *Neuropsychiatric Disease and Treatment*. **14**, 3289–3298, doi:
650 10.2147/NDT.S174083 (2018).
651 47. Melak, M., Plessner, M., Grosse, R. Actin visualization at a glance. *Journal of Cell Science*.
652 **130** (3), 525–530, doi: 10.1242/jcs.189068 (2017).
653 48. Adams, A.E.M., Pringle, J.R. Staining of actin with fluorochrome-conjugated phalloidin.
654 *Methods in Enzymology*. **194**, 729–731, doi: 10.1016/0076-6879(91)94054-G (1991).
655 49. Belin, B.J., Goins, L.M., Mullins, R.D. Comparative analysis of tools for live cell imaging of
656 actin network architecture. *BioArchitecture*. **4** (6), 189–202, doi:
657 10.1080/19490992.2014.1047714 (2014).

50. Wulf, E., Deboben, A., Bautz, F.A., Faulstich, H., Wieland, T. Fluorescent phallotoxin, a tool for the visualization of cellular actin. *Proceedings of the National Academy of Sciences of the United States of America*. **76**, 4498–4502, doi: 10.1073/pnas.76.9.4498 (1979).
51. Taffarel, M., de Souza, M.F., Machado, R.D., de Souza, W. Localization of actin in the electrocyte of Electrophorus electricus L. *Cell and Tissue Research*. **242**, 453–455, doi: 10.1007/BF00214562 (1985).
52. Glebov, O.O. Distinct molecular mechanisms control levels of synaptic F-actin. *Cell Biology International*. **44** (1), 336–342, doi: 10.1002/cbin.11226 (2020).
53. Dancker, P., Löw, I., Hasselbach, W., Wieland, T. Interaction of actin with phalloidin:. Polymerization and stabilization of F-actin. *BBA - Protein Structure*. doi: 10.1016/0005-2795(75)90196-8 (1975).
54. Lengsfeld, A.M., Löw, I., Wieland, T., Dancker, P., Hasselbach, W. Interaction of phalloidin with actin. *Proceedings of the National Academy of Sciences of the United States of America*. **71** (7), 2803–2807, doi: 10.1073/pnas.71.7.2803 (1974).
55. Coluccio, L.M., Tilney, L.G. Phalloidin enhances actin assembly by preventing monomer dissociation. *Journal of Cell Biology*. **99**, 529–535, doi: 10.1083/jcb.99.2.529 (1984).
56. Colicos, M.A., Collins, B.E., Sailor, M.J., Goda, Y. Remodeling of synaptic actin induced by photoconductive stimulation. *Cell*. **107** (5), 605–616, doi: 10.1016/S0092-8674(01)00579-7 (2001).
57. Lemieux, M.G. et al. Visualization of the actin cytoskeleton: Different F-actin-binding probes tell different stories. *Cytoskeleton*. **71**, 157–169, doi: 10.1002/cm.21160 (2014).
58. Bubb, M.R., Senderowicz, A.M.J., Sausville, E.A., Duncan, K.L.K., Korn, E.D. Jasplakinolide, a cytotoxic natural product, induces actin polymerization and competitively inhibits the binding of phalloidin to F-actin. *Journal of Biological Chemistry* (1994).
59. Holzinger, A. Jasplakinolide: an actin-specific reagent that promotes actin polymerization. *Methods in molecular biology (Clifton, N.J.)*. **269**, 14869–14871, doi: 10.1007/978-1-60761-376-3_4 (2009).

Figure 1

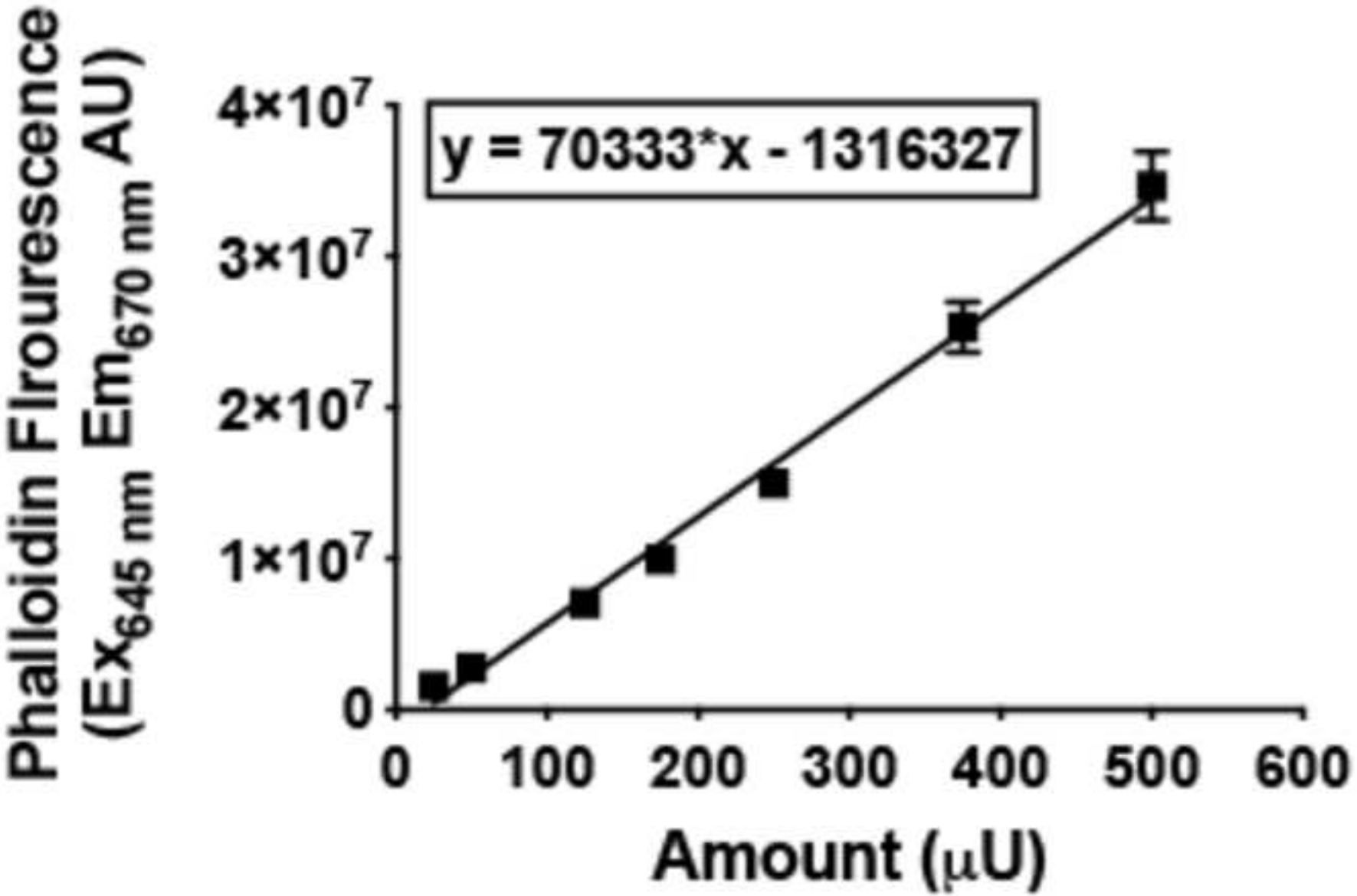

Figure 2

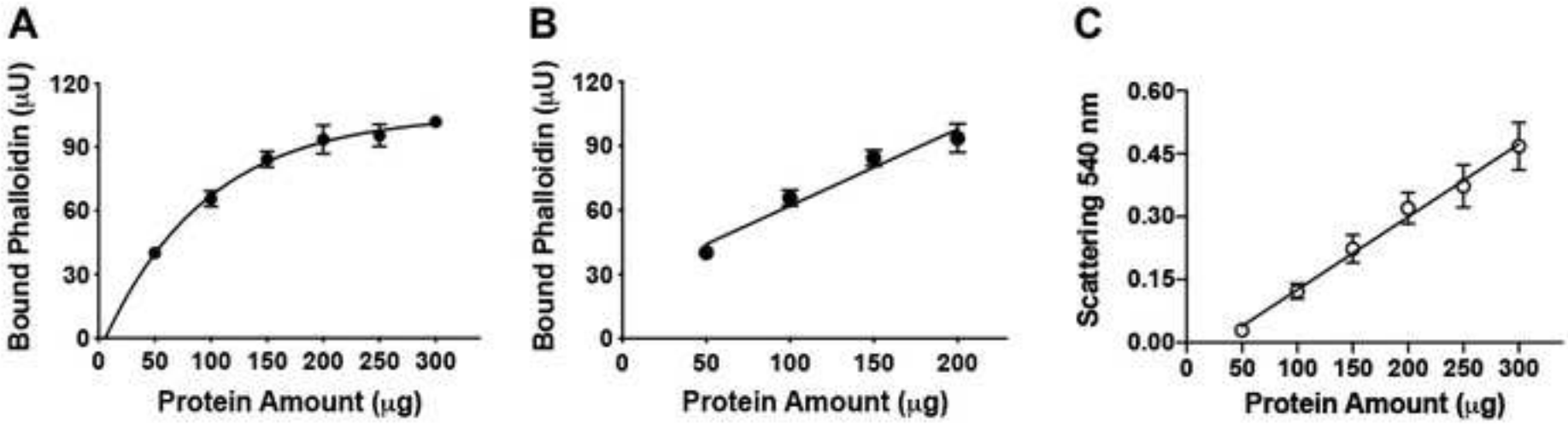

Figure 3

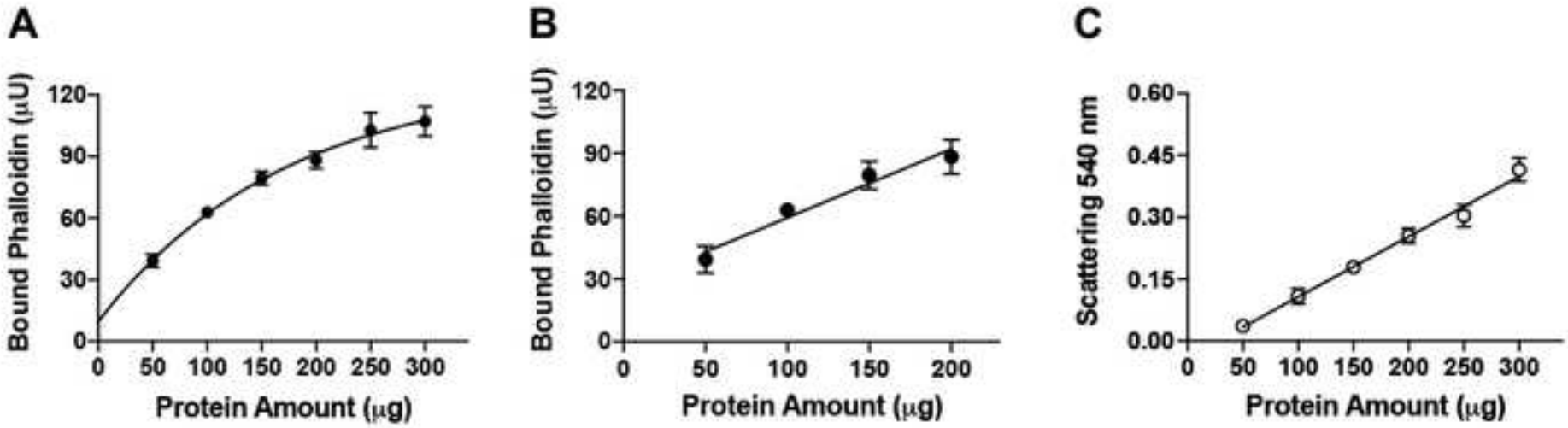

Figure 4

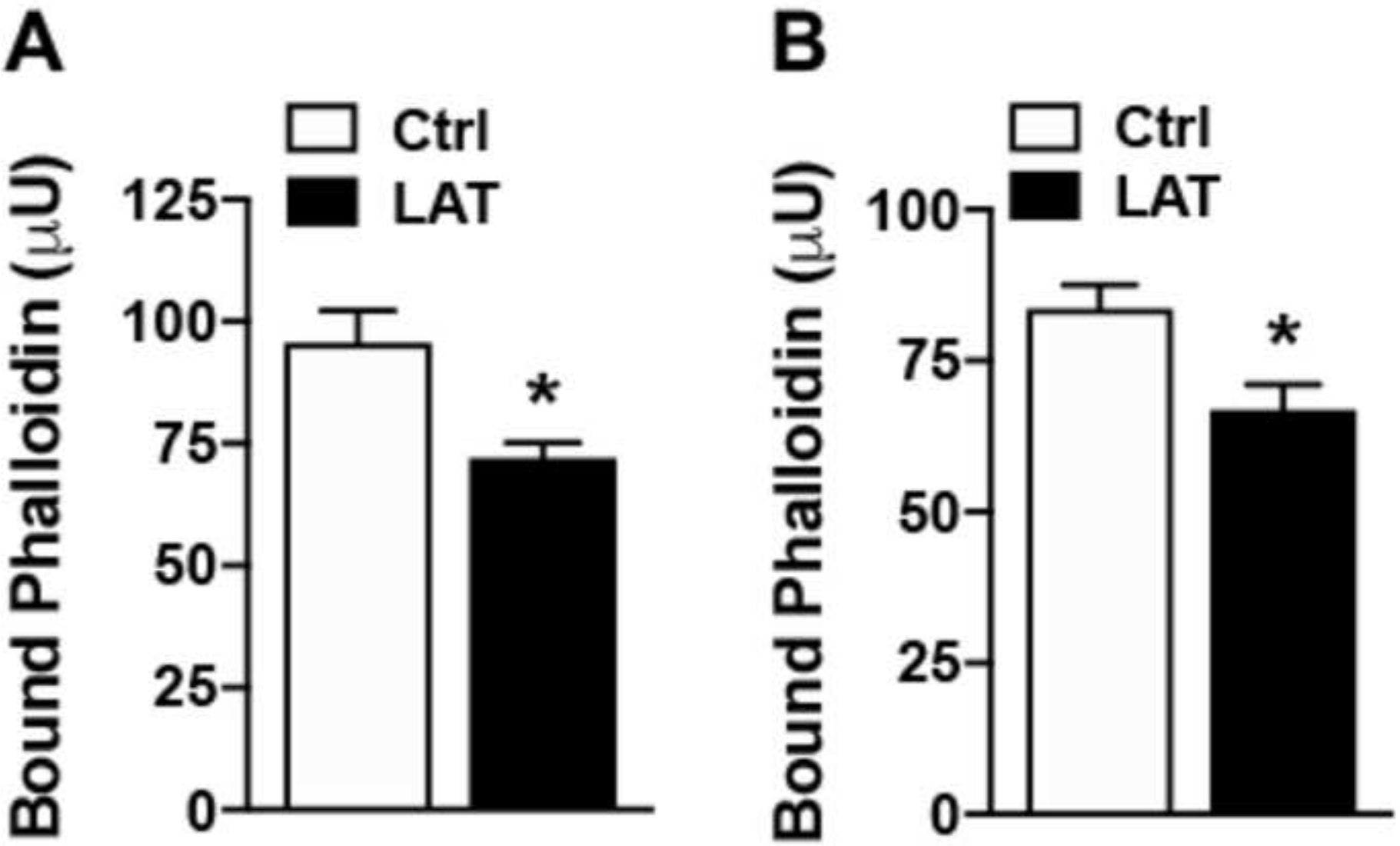

Figure 5

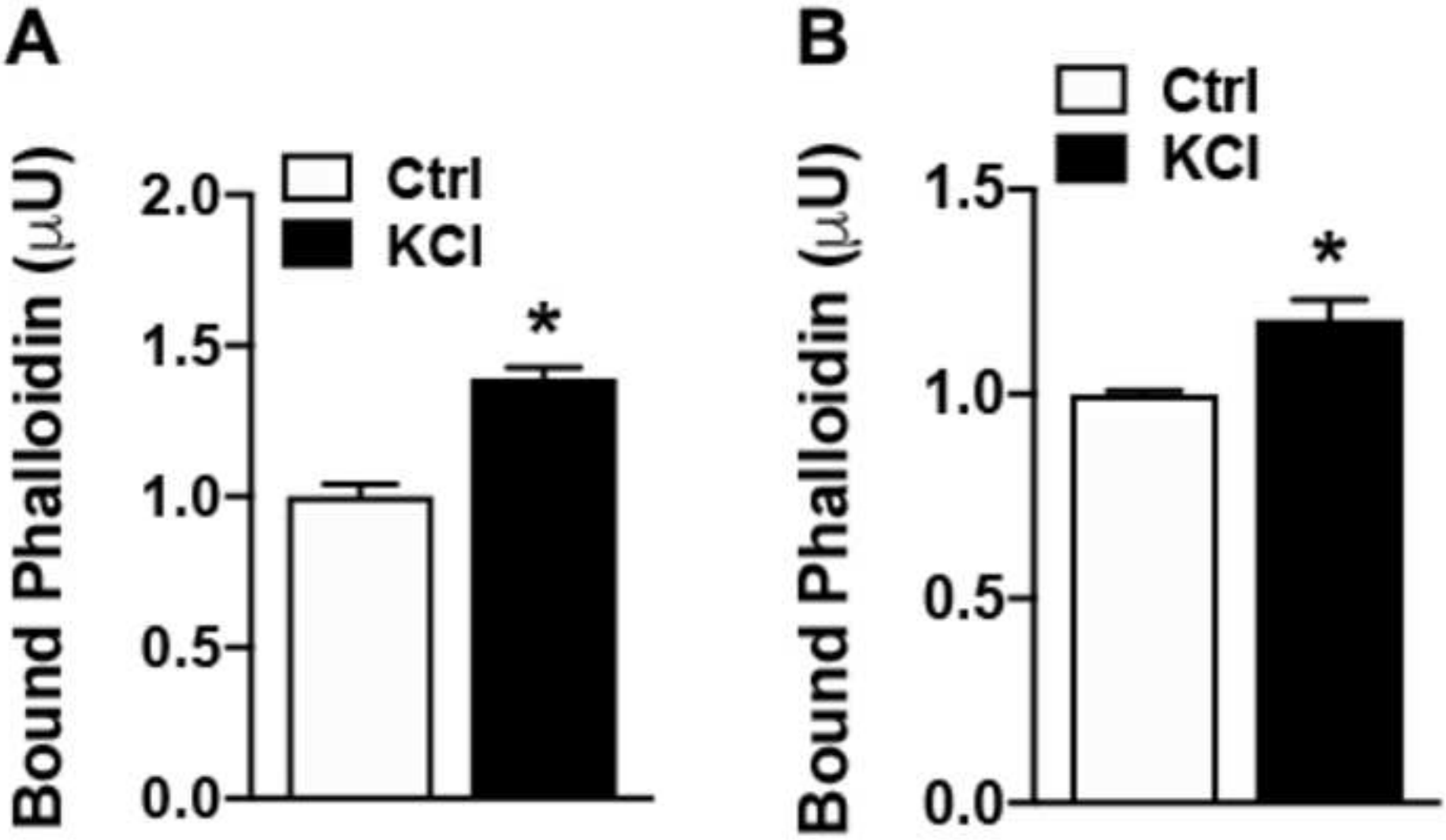

Table of Materials

Name of Material/Equipment	Company	Catalog Number	Comments/Description
3.5 mL, open-top thickwall polycarbonate tube	Beckman Coulter	349622	For gradient centrifugation (synaptosome prep)
Alexa Fluor 647 Phalloidin	Thermo Fisher Scientific	A22287	F-actin specific ligand
Antibody against β-actin	Santa Cruz Biotechnology	Sc-47778	For evaluation of total actin levels by immunoblotting
Antibody against GAPDH	Abcam	Ab181602	For evaluation of GAPDH levels by immunoblotting
Bio-Rad Protein Assay Dye Reagent Concentrate	Bio-Rad	5000006	Bradford based protein estimation
Calcium chloride dihydrate ($CaCl_2 \bullet 2H_2O$)	Sigma-Aldrich	C3306	Krebs buffer component
cOmplete, Mini, EDTA-free Protease Inhibitor Cocktail	Sigma-Aldrich	4693159001	For inhibition of endogenous protease activity during sample preparation
Corning 96-well Clear Flat Bottom Polystyrene	Corning	3596	For light-scattering measurements
D-(+)-Glucose	Sigma-Aldrich	G8270	Krebs buffer component
Dimethyl sulfoxide	Sigma-Aldrich	D5879	Solvent for phalloidin and latrunculin A
Fluorescent flatbed scanner (Odyssey Infrared Scanner)	Li-Cor Biosciences		For detection of immunoreactive signals on immunoblots
Glutaraldehyde solution (25% in water) Grade II	Sigma-Aldrich	G6257	Fixative
HEPES	Sigma-Aldrich	H3375	sample preparation and

Latrunculin A	Sigma-Aldrich	**L5163**	Depolymerizer of actin filaments
Magnesium chloride hexahydrate ($MgCl_2 \cdot 6H_2O$)	Sigma-Aldrich	M2670	Krebs buffer component
Microplates			
Mitex membrane filter 5 μm	Millipore	LSWP01300	Preparation of
Nunc F96 MicroWell Black Plate	Thermo Fisher	237105	For fluorometric
Nylon net filter 100 μm	Millipore	NY1H02500	Preparation of synaptoneurosomes
Phosphatase Inhibitor Cocktail IV	Abcam	ab201115	For inhibition of endogenous phosphatase activity during sample preparation
Potassium chloride (KCl)	Sigma-Aldrich	P9541	Krebs buffer component
Potassium phosphate monobasic	Sigma-Aldrich	P9791	Krebs buffer component
Sodium borohydride ($NaBH_4$)	Sigma-Aldrich	71320	Component of Permeabilization buffer
Sodium chloride (NaCl)	LabServ (Thermo	BSPSL944	Krebs buffer component
Sodium hydrogen carbonate	LabServ (Thermo	BSPSL900	Krebs buffer component
SpectraMax i3x	Molecular Devices		For fluorometric measurements
Sucrose	Fisher Chemical	S/8600/60	Buffer ingredient for
Swimnex Filter Holder	Millipore	Sx0001300	Preparation of
Tissue grinder 5 mL Potter-*Elvehjem*	Duran Wheaton Kimble	358034	For tissue homogenization
Triton X-100	Sigma-Aldrich	X100	Component of Permeabilization buffer
Trizma base	Sigma-Aldrich	T6066	Buffer ingredient for sample preparation

Dear Dr. Nguyen,

Please find attached the revised manuscript, JoVE62268 "A time-efficient fluorescence spectroscopy-based assay for evaluating actin polymerization status in rodent and human brain tissues," with the suggested additions and changes for both the text (in track-change mode) and the video.

Please also find attached below the rebuttal addressing each of the editorial and peer review comments individually.

Sincerely,

Faraz Ahmad

Editorial and production comments:
Changes to be made by the Author(s) regarding the written manuscript:
1. Please take this opportunity to thoroughly proofread the manuscript to ensure that there are no spelling or grammar issues.

Response:
We have revised the manuscript thoroughly in this respect and rectified the errors.

2. Please include an ethics statement before your numbered protocol steps, indicating that the protocol follows the animal care guidelines of your institution.

Response:
We have now included these additional information (see lines 109-114).

3. Please add more details to your protocol steps. Please ensure you answer the "how" question, i.e., how is the step performed?

Response:
We have now included these additional information.

4. 1.2: What concentrations of what are used?

Response:
We have now provided the concentrations used (see lines 126-127), which was according to the vendors' instructions.

5. 2.1: For how long? To what end point?

Response:
We have now included these additional information (see lines 152-154).

6. 2.2: Please provide a reference here.

Response:
We have now included the reference as suggested (see line 155).

7. Please specify the volumes used for the washings.

Response:
We have now specified the volumes used for the washings as suggested (see line 262).

8. Please specify all volumes used throughout.

Response:

We have now specified all volumes used throughout as suggested.

Changes to be made by the Author(s) regarding the video:

1. Please increase the homogeneity between the video and the written manuscript. Ideally, the narration is a word for word reading of the written protocol.

Response:

We have now increased the homogeneity between the video and the written manuscript as suggested and also made it more coherent with the main Figures 1-5.

2. Please identify all speakers with on screen text.

Response:

We have now done this.

3. The video says the cells were from rats or human. Please provide an ethics statement regarding the usage of both cell types in the video and the written manuscript.

Response:

We have now included the ethical information in the text and video as suggested.

4. Video

• Fade up from black at beginning of video
• Fade to black at end of video
• No cross-dissolves or fades have been used. Consider using dissolves to smooth transitions between clips within sections, and consider using fades (fade to white or black) to smooth transitions between sections.
• 03:37 - Edit out white frames
• 04:08 - Edit out white frames
• Please remove the entire shot of the commercial product: AlexaFluor
• 04:39 - There is a short clip that has been looped to fit the VO. Consider making this a still frame image or shooting a replacement clip.
• 05:24 - Give a second of pause between sections V and VI.

Response:

We have edited the video as suggested.

5. Audio

• Audio gain needs to be reduced by 6db
• Edit out any mouth clicking noises at the start of sentences.
• 04:43 - Sound of rustling paper is heard, edit this out.

Response:

We have edited the audio as suggested and hope it is fine now.

Reviewers' comments:

Reviewer #1:

The authors of this manuscript have developed a method to assess polymerization status of actin in ex vivo conditions. In the assay, F-actin is labelled by Phalloidin tagged with Alexa Fluor 647. The fluorescence intensity correlates with the used amount [µU] of Phalloidin-A647 (Fig.1) in unbound liquid phase. Therefore, measuring changes in fluorescence

intensity of different Phalloidin-AF647 stained samples is directly correlated with amount of labelled F-actin.
In principle, this is an interesting protocol and method which could help to analyze actin dynamics in samples with a medium throughput. However, there are some limitations:
1. The assay is clearly limited to low protein concentration samples since binding saturation occurs fast. Authors state that linearity of the read-out occurs between 50 and 200 µg of protein (Fig. 2B). However, the fitted data for a broader range (Fig. 2A) show that fluorescence at higher values is already becoming saturated. Authors use 500 µU for each sample. Highest amount of binding seems to be at 100 µU in the samples used (Fig. 2A, Fig.4A-B).

Response:

For our tissue type of interest (brain), the linear range of phalloidin retention (when its starting amount is 500 µU) is 50-200 µg. For the 50 µg sample, there may be more prominent variations in retention of the samples (lines 283-284). Hence, we suggest a working range of 100-150 µg of protein (Fig. 2B) for the assay for which 500 µU phalloidin is not limiting. Specifically, we used 100 µg for synaptosomes/synaptoneurosomes and 150 µg for homogenates mainly because of the lower yields of synaptosomes compared to homogenates and also because we expected to observe a decrease in the homogenate (treated with latrunculin A compared to mock treated samples) and an increase in synaptosomes (treated with KCl compared to mock treated samples). For other tissue types, optimal sample amounts and phalloidin concentrations should be determined.

The reviewer stated that "the assay is limited to low protein concentration samples". In fact, higher amounts of protein (even for brain samples) can be assessed using higher starting concentrations of phalloidin. Because human brain tissues are precious, we standardized the assay with the lowest amounts of samples without affecting the robustness of the assay (100-150 µg protein with a starting 500 µU phalloidin per sample). We have indicated this now in lines 266-268.

Further, for post-mortem human tissue authors did not check binding of phalloidin-A647 for the whole range of protein amount (0-300µg) (Fig. 3A). This leads to the proposed linearity of the assay which is in fact probably in the saturated range.

Response:

We did not test the higher amounts of proteins because human tissues are precious. However, upon the reviewer's request, we now checked the binding of phalloidin-A647 for the whole range of protein amount (50-300µg) of post-mortem human tissue (see lines 306-308 and lines 374-378), and present the new data in Fig. 3. Our data indicate binding efficiency of phalloidin in human homogenates is similar to rat brain homogenates.

2. The amount of protein used was determined by measuring light scattering at 540 nm. Of note, protein concentration determination at 540 nm with spectroscopy is done using the Biuret approach. Is this what they did?

Response:

No, we just measured the absorbance of the samples at 540 nm. Light scattering at this wavelength depends on the turbidity of the samples, representing a relative measure of sample amounts. We have retained this method for relative assessment of sample content of the fixed samples from the publication (Bernstein and Bamburg 1989, Neuron, 3:257-265) from which this study is modified from. Normal assays for

protein assessment such as Biuret or Bradford may not optimally work in glutaraldehyde-fixed samples because of the presence of excessively cross-linked proteins. We have also removed 'proteins' in the results section (see lines 310-311), figure legends (see lines 370-371 and 377) and discussion (lines 531-532) to avoid this confusion.

3. For the proof of principle, authors treated rodent and human samples with Latrunculin A, a strong actin depolymerizing drug and measured decrease of bound phalloidin-A647. Again, authors can show binding of phalloidin-A647 to F-actin in control and treated conditions (Fig. 4A+B). However, the biological mechanism for decrease in phalloidin-A647 binding is unclear. It is not clear whether the same amount of protein has been used for both conditions. Furthermore, to state the biological effect of Latrunculin A, a more suitable control, e.g. measuring whole actin (F+G) and calculating the fraction (F/(F+G)) is necessary.

Response:

We indeed used the same amount of material and incubation time for the respective treated (with latrunculin A) and untreated (with same volume of DMSO) samples. This has been clarified in the text now (see lines 160-164, 316-317 and 382-383). Please note that upon the request of reviewer 3, we have repeated the experiments and have new data with increased number of experimental pairs for Fig. 4.

Furthermore, to state the biological effect of Latrunculin A, a more suitable control, e.g. measuring whole actin (F+G) and calculating the fraction (F/(F+G)) is necessary.

Response:

We have now done this experiment and added the data showing no effect of latrunculin A treatment on total actin levels in homogenates (Supplementary Fig.1). Please note that for this experiment involving immunoblotting, we have taken a small amount (10 μg) of the samples just after latrunculin A treatment, prior to fixing (see lines 163-164).

Moreover, F-actin could be lost due to preparation of samples. If it is not possible to measure G-Actin, samples have to be treated exactly the same way during preparation and have to measured in parallel.

Response:

The experiments were done exactly as the reviewer indicates. Please see the response above and clarifications in lines 160-164, 316-317 and 382-383.

In this case, authors need to use a paired Students t-test instead of an unpaired t-test.

Response:

We thank the reviewer for pointing this out. We have now analysed the results using paired tests as suggested (lines 384-385).

4. The assay does work for specific isolated cellular fractions. Authors show in depolarized rodent synaptosomes and human synaptoneurosomes an increase of bound Phalloidin-A647 (Fig. 5A+B). Normalization in this experiment is completely different to normalization before. Authors set amount of bound phalloidin-A647 in controls to 1 and calculated amount of bound Phalloidin-A647 in treated samples as a ratio to the control. The amount of analyzed synaptosomes/synaptoneurosomes or protein amount should be measured to calculate the amount of F-Actin (same as for Fig. 4).

Response:

We have now added the new analyses in the absolute units of phalloidin bound (Supplementary Fig. 2) as requested. Please note that upon the request of reviewer 3, we have repeated the experiments and have new data with increased number of experimental pairs for Fig. 5.

Minor point:
Typos in figure labelling

Response:
We thank the reviewer for pointing this out. The errors have now been amended.

Reviewer #2:
Manuscript Summary:
The authors wrote a manuscript and produced a video on a quick and efficient fluorescence spectroscopy-based assay for evaluating actin polymerization status in brain tissue. They used this method in their published papers. The manuscript is well written, fluent and solid. The aim is decent. I also reviewed the video produced by the author. It is clear, easy to understand and accurate. Time in the video is associated with comments.

The authors report a fluorescence-based method to evaluate the polymerization status of actin in rodent and post-mortem human brain tissue homogenates. They demonstrate how to prepare synaptosomes and synaptoneurosomes, then depolarize the isolated synaptic terminals by KCl. After fixation, label the samples by fluorescent phalloidin. The fluorescently labelled phalloidin binds to F-actin, to provide a direct measurement of polymerized filamentous actin. F-actin levels in the samples are directly proportional to the fluorescence intensity of bound phalloidin. By using the drug latrunculin A that depolymerizes actin filaments, they showed that this method could detect changes in F-actin levels. They demonstrated an easy, fast assay for analysis of F-actin, and its alternations in physiological and pathophysiological states suitable for small amounts of samples.

The title and abstract is appropriate for this methods article. However instead of 'rodent and human brain tissues' only 'brain tissue' could be written.

Response:
We thank the reviewer for the time and efforts in assessing our work. We would like to keep the title as such, because we want to emphasize that our technique is suitable for measuring F-actin changes in homogenates and synaptosomes of human post-mortem brain tissues. This is essential because of the challenges associated with studying physiological processes such as actin dynamics using other methods (e.g. immunocytochemistry) in post-mortem brains of human subjects.

All the materials needed are listed in the manuscript.

I think, the steps listed in the procedure would lead to the described outcome.

The listed steps in the procedure are clearly explained, and I do not think any important steps are missing. The critical steps are highlighted.

Controls are included in the procedure. Representative results are given, and they are useful to readers.

My concerns are listed below:

The reference 'Ahmad F, Liu P. Synaptosome as a tool in Alzheimer's disease research. Brain Res. 2020 Nov 1;1746:147009. doi: 10.1016/j.brainres.2020.147009.' provided in the video is not given in the manuscript. Please add.

Response:

We thank the reviewer for pointing this out, and have now added the reference (line 331; ref 41).

Please provide the concentration for the mix of protease and phosphatase inhibitors.

Response:

We have now provided the concentrations used (lines 126-127).

In literature, it is seen that cold methanol is also used for rapid F-actin fixation. The sentence in line 361, 362 'For example, methanol fixation alter native F-actin conformation and hence should be avoided.' could be modified.

Response:

We agree with the reviewer that methanol is widely used as a fast fixative for F-actin. Since we have not ourselves tested its efficiency, we feel that it is better to remove the sentence.

The sentence 'Of note, recent studies indicate alterations in neuronal actin cytoskeleton as a key pathological event in a wide range of neuropathologies, including ageing-related neurodegeneration and neurodevelopmental diseases.' should be deleted from the abstract. It could be given in the introduction or discussion with its reference.

Response:

We have removed in this sentence from the abstract as suggested. We already had this information in the introduction (lines 74-77).

Reviewer #3:

Manuscript Summary:

The manuscript describes a fluorescent based technology to assess polymerisation status of actin extracted from brain tissue. This technic used fluorescent labelled phalloidin that selectively binds to filamentous actin to obtain a quantitive measure of the presence of F-actin in tissue. The protocol is well described with a step by step procedure that will be very useful for the reproduction of this assay. The pharmacological characterisation of the presence of increasing levels of F-actin in neurosynaptosomes exposed to depolarising conditions is convincing. The authors are ranging the level of polymerisation that has been described in living tissue in similar conditions.

Response:

We thank the reviewer for the time and efforts in assessing our work and the positive comments.

Major Concerns:

The relative modest effect of latrunculin (-25% of F-actin), a drug that should fully depolymerised filamentous actin in cell culture is puzzling. The authors should explained this discrepancy with previous results using similar pharmacological compound.

Response:

Depolymerization of F-actin is highly concentration dependent (Fujiwara et al. 2018, Current Biology, 28:3183-3192. In this study, we used a concentration of 2 μM

latrunculin A, which has been shown to reduce F-actin levels only modestly (20-30% decrease) in synaptosomes (Wolf et al. 2015, Cerebral Cortex, 25:2863-2875). In neuronal cultures also, a modest decrease in F-actin (phalloidin staining) was also seen even after prolonged incubation with 2.5 μM latrunculin A (Zhang and Benson 2001, Journal of Neuroscience, 21:5169-5181). On the other hand, much more prominent loss of F-actin is seen in neuronal colures treated with higher dose of latrunculin A (for example 10 μM; Merriam et al. 2013, Journal of Neuroscience, 33:16471-16482). Of note, previous studies and our own unpublished results have indicated that even lower concentrations of latrunculin A (100 nM, for example) do not alter the basal F-actin levels at all, but only inhibit the formation of new F-actin (Gu et al. 2010, Nature Neuroscience, 13:1208-1215; Yang et al. 2008, Proceedings of the of National Academy of Sciences of the USA, 105:11388-11393).

Minor Concerns:

The statistic test used are mostly paired t-test. Because of the relative small number of values analysed, I will be more confortable with non-parametric tests.

Response:

We have now repeated the experiments and increased the sample size to 6 pairs and the new data are presented in Figs. 4 and 5, and hope that the use of paired t-test is now justified. We have also assessed statistical significance using Wilcoxon matched-pairs signed rank test for the data and found that it also gives similar statistical difference between the groups.

It will be interesting that the authors justify the use of 645 nm wavelength to measure phalloidin binding.

Response:

The absorption maxima of Alexa Flour 647 phalloidin is at 645-650 nm and emission maxima at 668-671 nm. We chose 645 nm as the absorption wavelength and 670 as the emission wavelength. This allows a 25 nm difference between the two wavelengths that is suitable for some plate readers such as the one that we used (SpectraMax® i3x).

Supplemental Figure 1

Click here to access/download;Supplemental File (Figures, Permissions, etc.);Supplementary Fig.1.tif

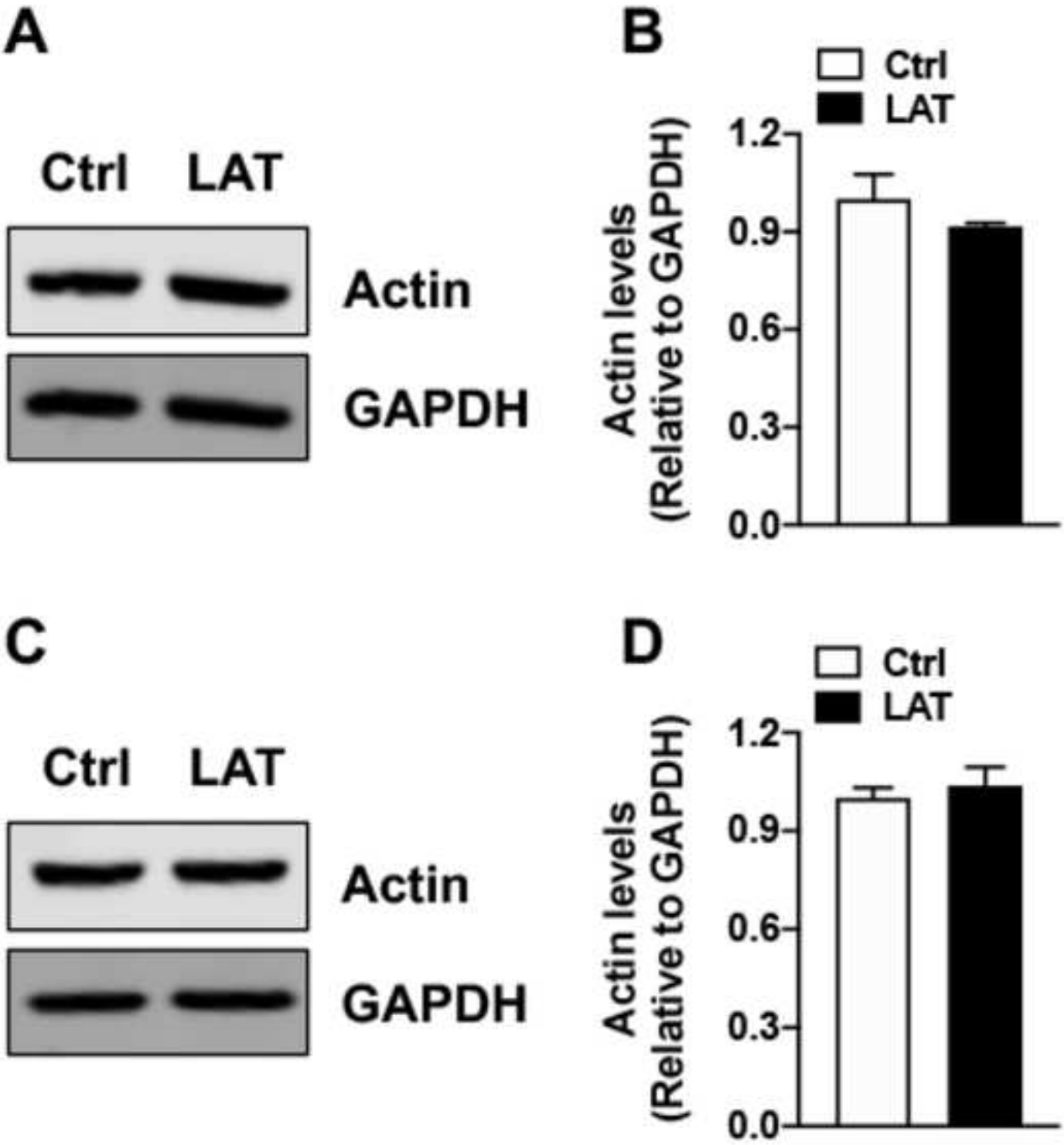

Supplemental Figure 2

Click here to access/download;Supplemental File (Figures, Permissions, etc.);Supplementary Fig.2.tif